Effect of Induced Spin-Orbit Coupling for Atoms via Laser Fields

Xiong-Jun Liu, Mario F. Borunda, Xin Liu and Jairo Sinova
Department of Physics, Texas A&M University, College Station, Texas 77843-4242, USA
(Dated: June 6, 2018)

We propose an experimental scheme to observe spin-orbit coupling effects of a two-dimensional (2D) Fermi atomic gas cloud by coupling its internal electronic states (pseudospins) to radiation in a Lambda configuration. The induced spin-orbit (SO) coupling can be of the Dresselhaus and Rashba type with and without a Zeeman term. We show that the optically induced SO coupling can lead to a spin-dependent effective mass under appropriate condition, with one of them able to be tuned between positive and negative effective masses. As a direct observable we show that in the expansion dynamics of the atomic cloud the initial atomic cloud splits into two clouds for the positive effective mass case regime, and into four clouds for the negative effective mass regime.

PACS numbers: 71.70.Ej, 37.10.Vz, 03.75.Ss, 05.30.Fk

Spin-orbit (SO) coupling effect in semiconductors has emerged in the solid-state community as a very active field of research, fuelled in part by the field of spintronics [1], e.g. the engineering of devices where the spin degree of freedom of the electron is exploited for improved functionality. This has lead to new developments in the anomalous Hall effect (AHE) [2] and the spin Hall effect (SHE) [3, 4]. In correspondence to the spin of an electron, the internal degree of freedom of an atom (pseudospin) is represented by the superposition of its electronic states (hyperfine levels). SO coupling can be equivalently depicted as the interaction between an effective non-Abelian gauge potential and a particle with (pseudo)spin. In quantum systems, the idea generating a gauge field adiabatically was proposed by Wilczek and Zee more than twenty years ago [5]. Recently, such an idea was applied to atomic systems, where the motion of atoms in a position dependent laser configuration gives rise to an effective non-Abelian gauge potential [6, 7, 8, 9, 10], which can lead to an effective SO interaction in an ultracold atomic gas [11, 12, 13].

Realization of SO interaction in atomic gases opens new possibility of studying spintronic effects, e.g. spin relaxation [11], *Zitterbewegung* [12] and SHE, in atomic systems which provide an extremely clean environment, allowing in a controllable fashion unique access to the study of complex physics. However, experimental detection of such SO effects in atoms requires to measure the pseudospins (not just hyperfine levels) that are usually not directly observable for atomic systems. In this letter, we propose an experimental scheme to study SO coupling effects, based on a trapped two-dimensional (2D) Fermi atomic gas with a simple internal three-level Λ-type setup. We demonstrate that an effective SO interaction, e.g. Rashba and linear Dresselhaus terms, can be obtained by coupling atoms with a three-level configuration to spatially varying laser fields. The optically induced SO coupling can lead to a spin-dependent effective masses under proper condition. A direct observable of this effects is in the expansion dynamics for each of the effective mass cases after the external trap is switched off and we predict that the initial atomic cloud splits into two or four clouds.

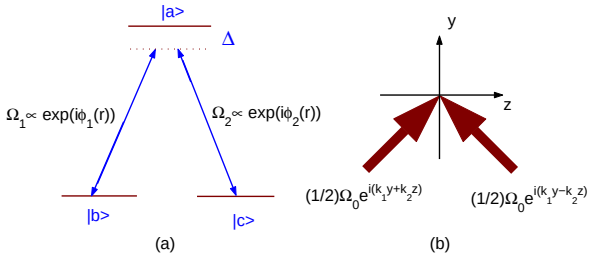

FIG. 1: (Color online) (a) Three-level Λ-type system coupled to position-dependent laser fields with large detuning; (b) Laser configuration for Ω_1.

We consider a cloud of quasi 2D (y-z plane) Fermi atomic gas with internal three-level Λ-type configuration (see Fig. 1 (a)) coupled to radiation. The transition $|b\rangle \to |a\rangle$ is coupled by the laser field with Rabi-frequency $\Omega_1 = \Omega_{10}\exp[i\phi_1(\mathbf{r})]$ and the transition $|c\rangle \to |a\rangle$ is coupled by another laser field $\Omega_2 = \Omega_{20}\exp[i\phi_2(\mathbf{r})]$, where $\phi_{1,2}(\mathbf{r})$ are position-dependent phases. The Hamiltonian of a single particle reads: $H = H_0 + V_{trap}(\mathbf{r}) + H_I$, where $V_{trap}(\mathbf{r})$ is the 2D harmonic trap, and the interacting Hamiltonian is given by

$$H_I = \hbar\Delta|a\rangle\langle a| - (\hbar\Omega_1|a\rangle\langle b| + \hbar\Omega_2|a\rangle\langle c| + h.c.). \quad (1)$$

Diagonalizing this Hamiltonian yields three eigenstates: $|\chi_D\rangle = \sin\theta|b\rangle - \cos\theta e^{i\phi}|c\rangle$, $|\chi_{B_1}\rangle = \cos\alpha\cos\theta|b\rangle + \cos\alpha\sin\theta e^{i\phi}|c\rangle + \sin\alpha e^{i\phi_1}|a\rangle$, and $|\chi_{B_2}\rangle = \sin\alpha\cos\theta|b\rangle + \sin\alpha\sin\theta e^{i\phi}|c\rangle - \cos\alpha e^{i\phi_1}|a\rangle$. Here $\phi = \phi_1 - \phi_2$, the mixing angles $\tan\theta = \Omega_{20}/\Omega_{10}$ and $\tan\alpha = \sqrt{\Omega_{10}^2+\Omega_{20}^2}/\Delta \equiv \Omega_0/\Delta$. The corresponding eigenvalues are $E_D = 0$ and $E_{B_{1,2}} = \hbar(\Delta \mp \sqrt{\Delta^2+4\Omega_0^2})/2$. Since spatially-varying lasers are employed, diagonalization of the interacting Hamiltonian H_I leads to a SU(3) gauge potential [6, 7, 8, 9]. We consider the large detuning case, $\Delta^2 \gg \Omega_0^2$, where $|E_D - E_{B_1}| \ll \Omega_0$ and $|\chi_D\rangle, |\chi_{B_1}\rangle$

spans a near-degenerate subspace, with their eigenvalues far separated from that of E_{B_2}. We can then apply the adiabatic condition by neglecting the state $|\chi_{B_2}\rangle$, which leads to a U(2) non-Abelian adiabatic gauge potential based on the near-degenerate subspace spanned by $|\chi_{D,B_1}\rangle$ [14]. This situation is different from the cases in Refs. 9 and 11 where the adiabatic condition is also assumed between the states $|\chi_D\rangle$ and $|\chi_{B_1}\rangle$, and thus the spin-dependent gauge potential is still Abelian in their case [9]. The adiabatic non-Ablelian gauge potential for the present near-degenerate subspace is obtained via

$$\mathbf{A}(\mathbf{r}) = i\frac{\hbar c}{e}\langle\chi_D| \otimes \langle\chi_{B_1}|\nabla|\chi_{B_1}\rangle \otimes |\chi_D\rangle. \quad (2)$$

For our purpose, we shall set the parameters $\phi_1 = \phi_2 = k_1 y$ and $\theta = k_2 z$, which means $\Omega_{1,2}$ are standing waves in the z direction but plane waves in the y direction. Such configuration can be achieved by applying two laser fields for each atomic transition. For Ω_1, for instance, we can set two laser fields with the same strength, where one travels with the wave vector $k_1\hat{e}_y + k_2\hat{e}_z$ and the other travels with $k_1\hat{e}_y - k_2\hat{e}_z$ (see Fig. 1 (b)), similarly can be done for Ω_2. The Rabi-frequencies are then given by $\Omega_1(\mathbf{r}) = \Omega_0\cos(k_2 z)e^{ik_1 y}$ and $\Omega_2(\mathbf{r}) = \Omega_0\sin(k_2 z)e^{ik_1 y}$. For simplicity, in what follows, we use the spin language and denote by $|\uparrow\rangle = |\chi_D\rangle$, $|\downarrow\rangle = |\chi_{B_1}\rangle$. Under this configuration the gauge field (2) can be recast into $\mathbf{A} = m\lambda_1\sigma_x\hat{e}_y - m\lambda_2\sigma_y\hat{e}_z - m\lambda_1 I\hat{e}_y$ with the coefficients $\lambda_1 = \hbar k_1\Omega_0^2/(2m\Delta_0^2)$ and $\lambda_2 = \hbar k_2/m$ (note $\mathbf{A}$ does not depend on mass m, and its current form is for the definition of $\lambda_{1,2}$). In addition, the scalar potentials are given by $\varphi_{\uparrow\uparrow} = \frac{\hbar^2}{2m}\frac{\Omega_0^2}{\Delta^2}k_2^2$, $\varphi_{\downarrow\downarrow} = \frac{\hbar^2}{2m}\frac{\Omega_0^2}{\Delta^2}k_1^2$, and $\varphi_{\downarrow\uparrow} = 0$.

To this step we can obtain the effective Hamiltonian for the near-degenerate subspace with SO coupling in the form (neglecting constant terms):

$$H = H_0 + H_{so} + H_z + V_{trap}, \quad (3)$$

where $H_0 = \frac{P_y^2}{2m} + \frac{P_z^2}{2m}$, $H_{so} = -\lambda_1\sigma_z P_y + \lambda_2\sigma_y P_z$, $H_z = M_0\sigma_z$ with $M_0 = \frac{\hbar^2}{4m}\frac{\Omega_0^2}{\Delta^2}k_2 + \hbar\frac{\Omega_0^2}{2\Delta}$, and the 2D harmonic trap $V_{trap} = \frac{1}{2}m\omega^2(y^2+z^2)$. A Hamiltonian of this form is predicted to give SHE [3] for $M_0 = 0$ and planar Hall effect [15] for $M_0 \neq 0$ in solid state systems.

The term $H_{so} + H_z$ can be readily diagonalized in the momentum space, $(H_{so}+H_z)^{diag} = \hbar\sqrt{(\frac{M_0}{\hbar} - \lambda_1 k_y)^2 + \lambda_2^2 k_z^2}\sigma_z$, where $k_{y,z}$ are wave vectors of atoms in the y and z directions. The associated eigenstates are given by $|+\rangle = [\cos\vartheta/2, i\sin\vartheta/2]^T$, $|-\rangle = [i\sin\vartheta/2, \cos\vartheta/2]^T$ with $\tan\vartheta = \lambda_2\hbar k_z/(M_0 - \lambda_1\hbar k_y)$. However, even in this situation, the full Hamiltonian H is not diagonalizable. Practically, we can consider the case where $M_0^2 \gg \lambda_2^2\hbar^2(k_F^z)^2 \gg \lambda_1^2\hbar^2(k_F^y)^2$ (the validity in realizable experimental set-ups will be discussed below), $k_F^{y,z}$ are the y/z-components of the Fermi momenta, and expand the term $(H_{so}+H_z)^{diag}$ to the k^2 order: $(H_{so}+H_z)^{diag} \approx (M_0 + \frac{\lambda_2^2 P_z^2}{2M_0} - \lambda_1 P_y)\sigma_z$. Substituting this result into eq. (3) yields

$$\begin{aligned} H^{(1)} &= \frac{1}{2m}(P_y - \lambda_1 m\sigma_z)^2 + \frac{1}{2\tilde{m}}P_z^2 + M_0\sigma_z \\ &\quad + \frac{1}{2}m\omega^2\mathbf{r}^2 - \frac{1}{2}m\lambda_1^2, \end{aligned} \quad (4)$$

where $\frac{1}{\tilde{m}} = \frac{1}{m} + \frac{\lambda_2^2}{M_0}\sigma_z$. Eq. (4) shows that the SO coupling leads to a spin-dependent effective mass of atoms moving in the z direction, with $\tilde{m}_\pm = (1 \pm \delta m/m)^{-1}m$ and $\delta m = \hbar^2 k_2^2/M_0$. The eigenfunction of Eq. (4) reads

$$\Psi^\eta_{n_y,n_z}(y,z) = \psi_{n_y}(\omega_y, y)\tilde{\psi}^\eta_{n_z}(\omega_z^\eta, z)e^{i\eta\lambda_1 m y/\hbar}|\eta\rangle, \quad (5)$$

with $|\eta\rangle = |\pm\rangle$. Here $\psi_{n_y}, \tilde{\psi}^\eta_{n_z}$ are harmonic oscillator wave functions. The eigenvalues are given by $E^\eta_{n_y,n_z} = (n_y + \frac{1}{2})\hbar\omega_y + (n_z + \frac{1}{2})\hbar\omega_z^\eta + \eta M_0 - \frac{1}{2}m\lambda_1^2$, where $\omega_y = \omega$, $\omega_z^\eta = \omega\sqrt{1 + \eta\delta m/m}$ are spin-dependent effective trap frequencies due to SO coupling, and n_y, n_z are integers.

The results (4) and (5) are valid for the situation $\delta m < m$, where the effective mass of particles in state $|-\rangle$ is positive, i.e. $\tilde{m}_- > 0$. On the other hand, the negative effective mass regime for the $|-\rangle$ state can be reached when $\delta m > m$. In this case one can verify the dispersion relation $\varepsilon_k^- = H_0 + H_{so}^{(-)} + H_z^{(-)}$ (for atoms in $|-\rangle$) represents a double-well potential in the k_z axis, therefore a higher-order expansion with momentum k_z is required to derive the effective Hamiltonian. Similarly, we consider that $\lambda_2^4\hbar^4(k_F^z)^4 \ll M_0^4$ and can then expand ε_k^- up to the k_z^4 order, which gives a double well ϕ^4-type potential form in k_z-momentum space ($\tilde{m}_- < 0$), i.e. $\varepsilon_{k_z}^- = \frac{\lambda_2^4}{8M_0^3}P_z^4 + \frac{1}{2\tilde{m}_-}P_z^2$ [16]. Higher-order terms in the expansion can equivalently lead to small corrections to the coefficients of k_z^2 and k_z^4 terms. Finally we get effective Hamiltonian for atoms at state $|-\rangle$:

$$\begin{aligned} H_-^{(2)} &= \frac{1}{2m}(P_y + \lambda_1 m)^2 + \frac{\lambda_2^4}{8M_0^3}(1+\gamma_1)P_z^4 \\ &\quad + \frac{1}{2\tilde{m}_-}(1+\gamma_2)P_z^2 - M_0 + \frac{1}{2}m\omega^2\mathbf{r}^2 - \frac{1}{2}m\lambda_1^2 \end{aligned} \quad (6)$$

Here the coefficient correction $\gamma_1 = \frac{4}{\frac{\delta m}{m}(1+\frac{\delta m}{m})^2} - 1, \gamma_2 = \frac{2}{1+\frac{\delta m}{m}} - 1$ are small under the condition $\lambda_2^4\hbar^4(k_F^z)^4 \ll M_0^4$, say, $\gamma_{1,2}^2 \ll 1$ in the present case.

Unlike the positive mass regime, calculation of the Fermi energy in the negative mass case cannot be done analytically. Nevertheless, we are interested in systems with a large number of atoms, where the Thomas-Fermi (TF) approximation is suitable [17, 18, 19]. Then the Fermi energy can be calculated by solving the equation:

$$N = \sum_{\eta=+,-}\int_{k<k_F^\eta, r<R_F^\eta} d^2\mathbf{r}d^2\mathbf{k}\rho_\eta^{(2)}(\mathbf{r},\mathbf{k},T=0), \quad (7)$$

where the atomic distribution function in phase space is given by $\rho_\pm^{(2)} = (2\pi)^{-2}(e^{\beta(H_\pm^{(2)}(\mathbf{r},\mathbf{k})-\mu_F)} + 1)^{-1}$ with

$\beta = 1/k_BT$, and the initial size of the atomic cloud is given by $R_F^{\pm} = (2\varepsilon_F \mp 2M_0 - 2\min\{\varepsilon_{k_z}^{\pm}\})^{1/2}/(m^{1/2}\omega)$. From Eq. (7) the relation of Fermi energy to the number of atoms N, trap frequency and SO coupling strength can be obtained numerically as shown in Fig.2.

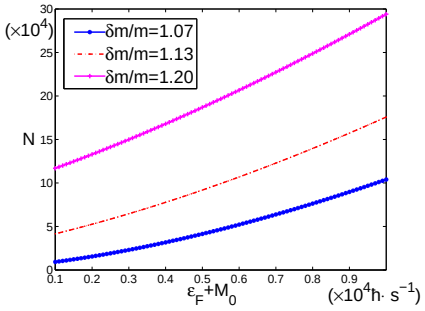

FIG. 2: (Color online) Number of atoms versus Fermi energy at $\delta m/m = 1.07, 1.13, 1.20$, corresponding to the effective mass $\tilde{m}_- = -15m, -7.7m, -5m$.

There are specific observables of this spin-dependent effective mass induced by the spin-orbit coupling. Firstly, the anisotropy of the effective mass can lead to the anisotropic momentum distribution. Considering the Thomas-Fermi approximation, at zero temperature and for the positive mass case, the momentum distribution is given by $n_\pm(\mathbf{k}) = \frac{1}{2\pi m\omega^2}\big[\varepsilon_F \mp M_0 - \frac{\hbar^2}{2m}(k_y^2 + \frac{m}{\tilde{m}_\pm}k_z^2)\big]$. This contrasts with the result for the usual isotropic mass, where the atomic distribution in the momentum space is always isotropic irrespective of the shape of the trap [17]. For the negative effective mass case, $n_+(\mathbf{k})$ has the same form, while $n_-(\mathbf{k}) = \frac{1}{2\pi m\omega^2}\big[\varepsilon_F + M_0 - \frac{\hbar^2}{2m}(k_y^2 + \frac{m}{\tilde{m}_-}(1+\gamma_2)k_z^2 + \frac{m\lambda_2^4\hbar^2}{4M_0^3}(1+\gamma_1)k_z^4)\big]$. Also, a fully polarized Fermi gas is obtained when $\varepsilon_F < M_0$, and $n_+(\mathbf{k}) = 0$. The anisotropy of the momentum distribution can lead to anisotropy of the Fermi velocity in the y-z plane. For instance, when $\delta m/m = 3/4$ and $\varepsilon_F < M_0$, we have $v_F^z \approx v_F^y/2$. The anisotropy of Fermi velocity can be directly detected by time-of-flight absorption [18, 19].

However, the dramatic signature of SO effects in the present Fermi atomic gas resides in the expansion dynamics of the atomic cloud after the 2D external trap and the laser fields are switched off. The evolution of the atomic distribution in phase space $\rho(\mathbf{r}, \mathbf{k}, T, t)$ can be calculated by the Boltzmann transport equation assuming that at $t = 0$, $V_{trap} \to 0$ and $M_0 \to 0$. For the present cold dilute non-interacting Fermi gas, the evolution of $\rho_{b,c}(\mathbf{r}, \mathbf{k}, T, t)$ is followed by the ballistic law $\rho_{b,c}(\mathbf{r}, \mathbf{k}, T, t > 0) = \rho_{b,c}(\mathbf{r} - \hbar\mathbf{k}t/m, \mathbf{k}, T, 0)$ (here $|\mathbf{k}, \nu\rangle, (\nu = b, c)$ are the eigenstates after the trap and laser fields are turned off). The temporal atomic spatial density can be calculated by: $n_{b,c}(\mathbf{r}, T, t) = \int d^2\mathbf{k}\rho_{b,c}(\mathbf{r} - \hbar\mathbf{k}t/m, \mathbf{k}, T, 0)$. The eigenstates $|\mathbf{k}, \alpha\rangle, (\alpha = b, c)$ are related to the initial pseudospin basis $|\pm\rangle$ by $|\mathbf{k}, b\rangle \approx \frac{1}{2}|\mathbf{k} + k_2\hat{e}_z, +\rangle + \frac{1}{2}|\mathbf{k} - k_2\hat{e}_z, +\rangle + \frac{1}{2i}|\mathbf{k} + k_2\hat{e}_z, -\rangle - \frac{1}{2i}|\mathbf{k} - k_2\hat{e}_z, -\rangle$, and $|\mathbf{k}, c\rangle \approx \frac{1}{2}|\mathbf{k}+k_2\hat{e}_z, -\rangle + \frac{1}{2}|\mathbf{k}-k_2\hat{e}_z, -\rangle - \frac{1}{2i}|\mathbf{k}+k_2\hat{e}_z, +\rangle + \frac{1}{2i}|\mathbf{k} - k_2\hat{e}_z, +\rangle$. We find that the atomic density is:

$$n_b(\mathbf{r}, T, t) = \sum_{\eta=\pm}\int \frac{d^2\mathbf{k}}{4}\Big\{\rho_\eta^{(j)}[\mathbf{r} - \frac{\hbar t}{m}(\mathbf{k} + \eta k_2\hat{e}_z), \mathbf{k}, T, 0] + \rho_\eta^{(j)}[\mathbf{r} - \frac{\hbar t}{m}(\mathbf{k} - \eta k_2\hat{e}_z), \mathbf{k}, T, 0]\Big\}, \quad (8)$$

where $\rho_\pm^{(j)}(\mathbf{r}, \mathbf{k}, T, 0)$ denote the distribution functions for atoms in the state $|\pm\rangle$ for the positive mass ($j = 1$) and negative mass ($j = 2$) cases. The function $n_c(\mathbf{r}, T, t)$ can be calculated in the same way. Practically, we can assume that before the expansion begins $\varepsilon_F < M_0$, and then $\rho_+^{(j)}(r, \mathbf{k}, T, 0) = 0$. For the positive mass case, the evolution of the atomic density can be calculated exactly:

$$n_b(\mathbf{r}, T, t) = \frac{\sqrt{m\tilde{m}_-}}{8(1+\omega^2t^2)\beta\pi\hbar^2}\Big(\frac{1+\omega^2t^2}{1+\frac{\tilde{m}_-}{m}\omega^2t^2}\Big)^{1/2} \times\Big(\ln\frac{1+e^{-\beta\tilde{E}_+(\mathbf{r},t)}}{e^{-\beta\tilde{E}_+(\mathbf{r},t)}} + \ln\frac{1+e^{-\beta\tilde{E}_-(\mathbf{r},t)}}{e^{-\beta\tilde{E}_-(\mathbf{r},t)}}\Big), \quad (9)$$

where $\tilde{E}_\pm(\mathbf{r}, t) = \mu_F + M_0 - \frac{m\omega^2y^2}{2(1+\omega^2t^2)} - \frac{m\omega^2(z\pm\hbar k_2t/m)^2}{2(1+\frac{\tilde{m}_-}{m}\omega^2t^2)}$. One can verify that at $t = 0$ the maximum point of n_b is obtained at $\mathbf{r} = 0$, while after a sufficiently long time there are two maximum points at $y = 0, z = \pm\hbar k_2t/m$. As a result, Eq. (9) represents an initial atomic cloud that splits into two clouds each moving in opposite direction with group velocities $v_g = \pm\hbar k_2\hat{e}_z/m$. Using typical parameters: $M_0 = 10^6\hbar\cdot s^{-1}, m \approx 0.963\times10^{-26}kg$ (^{6}Li atoms) and $k_2 = 0.87\times10^7\mathrm{m}^{-2}$, one finds $\tilde{m}_- \approx 4m$, and $v_g \approx \pm9.0cm/s$.

The evolution of the atomic density in the negative effective mass regime is more complicated. Again, assuming $\varepsilon_F < M_0$, we find from Eq. (8) the temporal atomic density as (denoting by $\tilde{z}_\eta = z \pm \hbar k_2t/m$):

$$n_b(\mathbf{r}, T, t) = \sum_{\eta=+,-}\int\frac{d^2\mathbf{k}}{16\pi^2}\Big\{1 + \exp\big\{\beta[\frac{1+\omega^2t^2}{2m}\hbar^2k_y^2 + \frac{\Gamma}{2m\hbar^2}\big(\hbar k_z + \frac{\tilde{m}_-\omega^2t\tilde{z}_\eta}{1+\frac{\tilde{m}_-}{m}\omega^2t^2}\big)^4 + \frac{m+\tilde{m}_-\omega^2t^2}{2m\tilde{m}_-}\hbar^2k_z^2 + \frac{m\omega^2y^2}{2+2\omega^2t^2} + \frac{m^2\omega^2\tilde{z}_\eta^2}{2m+2\tilde{m}_-\omega^2t^2} - M_0 - \mu_F]\big\}\Big\}^{-1} \quad (10)$$

where $\Gamma = m\lambda_2^4\hbar^2(1+\gamma_1)/(4M_0^3)$. To make a qualitative analysis, we first calculate the time independent momentum distribution: $n_b(\mathbf{k}, T, t) = \frac{1}{8\pi m\omega^2}(\ln\frac{1+e^{-\beta\tilde{\mathcal{E}}_+(\mathbf{k})}}{e^{-\beta\tilde{\mathcal{E}}_+(\mathbf{k})}} + \ln\frac{1+e^{-\beta\tilde{\mathcal{E}}_-(\mathbf{k})}}{e^{-\beta\tilde{\mathcal{E}}_-(\mathbf{k})}})$. Here $\tilde{\mathcal{E}}_\pm(\mathbf{k}) = \mu_F + M_0 + \frac{\hbar^2\Gamma\Upsilon^2}{2m} - \frac{\hbar^2}{2m}\big[k_y^2 + \Gamma\big((k_z \pm k_2)^2 - \Upsilon\big)^2\big]$ with $\Upsilon = -m(1+\gamma_2)/(2\tilde{m}_-\Gamma)$. Note that if $k_2 \neq \sqrt{\Upsilon}$, $n_b(\mathbf{k}, T, t)$ has four distinct maximums at: $k_z = -k_2 - \sqrt{\Upsilon}$, $-k_2 + \sqrt{\Upsilon}$, $k_2 - \sqrt{\Upsilon}$, $k_2 + \sqrt{\Upsilon}$, which indicates that the initial atomic cloud is composed of four overlapping clouds that will travel in the z-axis

at different speeds. Using parameters similar to the previous system: $m \approx 0.963 \times 10^{-26} kg$ (^{6}Li atoms), $k_2 = 1.0 \times 10^7 \mathrm{m}^{-1}$, and $M_0 = 0.90 \times 10^6 \hbar \cdot s^{-1}$, we find that $\Gamma \approx 4.43 \times 10^{-15} \mathrm{m}^2$ and $\Upsilon = 8.9 \times 10^{12} \mathrm{m}^{-2}$. Thus the four maximums correspond to $v_g = \pm 13.4 cm/s, \pm 7.4 cm/s$.

Figure 3 displays numerical estimates of the splitting. The time at which such splitting can be observed is found by estimating the initial size of the atomic cloud, R_F. For system with $N \approx 10^{4\sim5}$ atoms and a trap frequency $\omega \sim$ 35HZ, $R_F \approx 230 \mu m$ in the positive effective mass case and $R_F \approx 127.8 \mu m$ when the effective mass is negative, assuming $T < T_F$. As a result, for the positive effective mass regime, one can verify that the two atomic clouds will be fully separated after the system evolves by $\Delta t \sim 5ms$. For the negative mass regime, the time is about $\Delta t \sim 9ms$. It should be emphasized that measurement of the present expansion dynamics needs to detect the density of atoms in the hyperfine level $|b\rangle$ (or $|c\rangle$), rather than to detect the pseudospin states $|\pm\rangle$ that are not differentiable for the atomic system, thus the SO effect obtained here is directly observable in experiments by direct imaging of the separated atomic clouds.

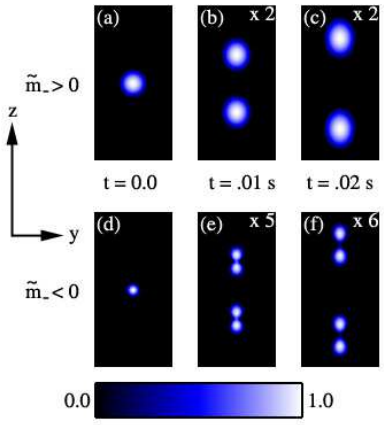

FIG. 3: (Color online) Splitting of atomic cloud for the positive effective mass case (a-c) and negative mass case (d-f) after turning off the trap and laser fields. The x n label represents the value each panel has been multiplied by to keep figure to scale.

Now we confirm the validity of the approximation $M_0^2 \gg \lambda_2^2 \hbar^2 (k_F^z)^2 \gg \lambda_1^2 \hbar^2 (k_F^y)^2$. The second inequality is always valid, since $\lambda_2 \gg \lambda_1$ in the large detuning case. Note that k_F^z can be calculated by $k_F^z = \sqrt{\Upsilon + 2m(\tilde{\varepsilon}_F + \hbar^2 \Gamma \Upsilon^2 / 2m)/(\hbar^2 \Gamma)}$ for $\tilde{m}_- < 0$ and $k_F^z = \sqrt{2\tilde{m}_- \tilde{\varepsilon}_F / \hbar^2}$ for $\tilde{m}_- > 0$. For the system composed of $N \sim 10^4$ atoms and a trap frequency $\omega = 35$HZ, and using the previously employed parameters, we find $k_F^z \approx 1.41 \times 10^6 m^{-1}$ with $\lambda_2^2 \hbar^2 (k_F^z)^2 / M_0^2 \approx 0.019 \ll 1$ for $\tilde{m}_- > 0$, and $k_F^z \approx 3.55 \times 10^6 m^{-1}$ with $\lambda_2^4 \hbar^4 (k_F^z)^4 / M_0^4 \approx 0.028 \ll 1$ for $\tilde{m}_- < 0$ (note for the case $\tilde{m}_- < 0$ the approximation is up to the k_z^4 order). Thus, the first inequality is also valid. Finally we estimate the TF approximation that is considered in the calculation. TF approximation fails in a small periphery region $R_F - \delta R < r < R_F$ of the atomic cloud [17]. For the 2D fermi atom gas, one can find the ratio of δR to the atomic cloud size R_F satisfies $\delta R / R_F \sim N^{-1/2}$. Therefore such a small region can be safely neglected for the case with a large number of atoms, say $N > 10^4$. Note this model can be readily extended to Bose-Einstein condensate systems [21], where, together with the atom-atom interaction, the SO coupling may lead to intriguing new physics.

In conclusion, we have proposed an experimental scheme to study SO coupling effects for a cloud of a 2D trapped Fermi gas. Under certain conditions, the optically induced SO coupling in atoms leads to a spin-dependent effective mass which can be positive or negative. In the expansion dynamics of the atomic cloud after switching off the trap, it is shown that the initial atomic cloud splits into two or four clouds moving oppositely depending on tunable spin-orbit coupling parameters. The present scheme provides an applicable way to directly observe the SO coupling in cold Fermi atoms.

We gratefully acknowledge discussions with V. Galastki. This work was supported by ONR under Grant No. onr-n000140610122, by NSF under Grant No. DMR-0547875, and by SWAN-NRI. Jairo Sinova is a Cottrell Scholar of the Research Corporation.

[1] S. A. Wolf *et al.*, Science **294**, 1488 (2001).
[2] T. Jungwirth *et al.*, Phys. Rev. Lett. **88**, 207208 (2002).
[3] S. Murakami *et al.*,Science **301**, 1348 (2003); J. Sinova *et al.*, Phys. Rev. Lett. **92**, 126603 (2004).
[4] Y. K. Kato *et al.*, Science, **306**, 1910 (2004); J. Wunderlich *et al.*, Phys. Rev. Lett. **94**, 047204 (2005).
[5] F. Wilczek and A. Zee, Phys. Rev. Lett. 52, 2111 (1984).
[6] J. Ruseckas *et al.*, Phys. Rev. Lett. **95**, 010404 (2005).
[7] K. Osterloh *et al.*, Phys. Rev. Lett. **95**, 010403 (2005).
[8] X. -J. Liu *et al.*,Phys. Rev. Lett. **98**, 026602 (2007).
[9] S.-L. Zhu *et al.*,Phys. Rev. Lett. **97**, 240401 (2006).
[10] Yong Li, *et al.*, Phys. Rev. Lett. **99**, 130403 (2007).
[11] T. D. Stanescu, C. W. Zhang, and V. Galitski, Phys. Rev. Lett. **99**, 110403 (2007).
[12] J.Y. Vaishnav *et al.*, Phys. Rev. Lett. **100**, 153002 (2008).
[13] A. M. Dudarev et al., Phys. Rev. Lett. **92**, 153005 (2004).
[14] Note that in the large detuning case both the states $|\chi_{D,B_1}\rangle$ decouple from the excited state $|a\rangle$ since $\sin\alpha \ll 1$, and then the decay of them is negligible.
[15] H. X. Tang *et al.*, Phys. Rev. Lett. **90**, 107201, (2003).
[16] Y. Shin, Experiments with Bose-Einstein Condensates in a Double-Well Potential, Doctoral Thesis, MIT, 2005.
[17] D. A. Butts and D. S. Rokhsar, Phys. Rev. A, **55**, 4346 (1997).
[18] B. DeMarco and D. S. Jin, Science, **285**, 1703 (1999).
[19] S. R. Granade *et al.*, Phys. Rev. Lett. **88**, 120405 (2002).
[20] R. Grimm *et al.*, Advances in Atomic, Molecular and Optical Physics Vol. 42, 95 (2000).
[21] T. Stanescu *et al.*, Phys. Rev. A **78**, 023616 (2008).